Full-Scale Aircraft Impact Test for Evaluation of Impact Forces
Part 1: Test Plan, Test Method, and Test Results

W. A. von Riesemann, R. L. Parrish, D. C. Bickel, S. R. Heffelfinger
Sandia National Laboratories, Albuquerque, NM USA
Kiyoshi Muto, Tadashi Sugano, Haruji Tsubota Norihide Koshika, Masayasu Suzuki, Satoshi Ohrui
Muto Institute of Structural Mechanics, Inc., Tokyo, Japan

1 INTRODUCTION

One of the factors considered in the design of critical concrete structures is the estimation of the global elasto-plastic structural response caused by the accidental impact of an aircraft. To estimate the response of the structure, the impact force (the force versus time relationship) must be known.

Previous analytical studies [1-4] have derived the forcing function using the impact velocity of the aircraft and the calculated mass and strength distribution of the aircraft. This paper describes a test conducted on April 19, 1988, at an existing rocket sled facility at Sandia National Laboratories in Albuquerque, New Mexico, USA, in which an actual F-4 Phantom aircraft was impacted at a nominal velocity of 215 m/s into an essentially rigid block of concrete. This was accomplished by supporting the F-4 on four struts that were attached to the sled track by carriage shoes to direct the path of the aircraft. Propulsion was accomplished by two stages of rockets. The concrete target was 'floated' on a set of air bearings. Data acquisition consisted of measurements of the acceleration of the fuselage and engines of the F-4, and measurements of the displacement, velocity and acceleration of the concrete target. High-speed photography recorded the impact process and also permitted the determination of the impact velocity.

This paper describes the test plan, method and results, while a companion paper [5] discusses the analyses of the results.

2 TEST PLAN

The primary purpose of the test was to determine the impact force versus time due to the impact of a complete F-4 Phantom onto a massive, essentially rigid reinforced concrete target. The impact velocity of 215 m/s corresponds to that of the full-scale engine tests performed previously [6]. The impact orientation was assumed to be head-on; i.e., normal to the target. Additional objectives of the test were: a) to determine the crush behavior of the aircraft, b) to determine if the engines were detached from the aircraft before their impact, and if so, to measure their impact velocity, and c) to record the dispersal of the 'fuel' after impact (water was used instead of fuel).

---

*At present the contact institute is Kobori Research Complex, Inc., Tokyo, Japan.

An extensive suite of diagnostic and response measurements was acquired. The aircraft velocity was determined by high-speed photography and a break-rod system on the sled track. The reduction in velocity of the aircraft fuselage and the engines during the impact sequence was determined from on-board acceleration measurements. The acceleration, velocity, and displacement of the target were measured with kinematic sensors. Breakwire systems and high-speed photography were employed to ascertain if the engines broke free from their mounts. Photographic coverage of the aircraft travel along the sled track and the impact sequence was obtained with 4 tracking cameras and 16 high-speed framing cameras.

The physical damage incurred during the test was assessed by measurements of the dispersion of the simulated fuel, measurements of the location of fragments of the aircraft, and mapping of the damage to the test panel.

3 TEST METHOD

An existing 600 m-long two-rail rocket sled facility that has a back-up structure for mounting test panels was used to perform the test. This facility has been used in conducting many tests, such as impact of spent-fuel shipping casks, turbine missiles and turbojet engines [6]. Knowledge gained from many previous tests permits a close control on the impact velocity.

A flyable F-4D aircraft was acquired by Sandia. The aircraft was modified slightly in order to support the aircraft at four locations with a special carriage structure (Figure 1). The carriage structure had shoes that were wrapped around the flanges of the rails to prevent lift-off and to guide the aircraft. As acquired, the aircraft weighed 12.7 tonnes (with some avionics removed). The impact weight was 19.0 tonnes, which included the weight of five rocket casings and 4.8 tonnes of water that was added to simulate the fuel weight and at the same time provide the proper mass distribution. The mass distribution of the F-4D, as configured for the impact test, is shown in Figure 2, while the mass distribution for an 'original' F-4D is shown in Figure 3.

Propulsion was provided by a two-stage rocket system in order to keep the maximum accelerations within the structural limits of the attachment points of the carriage system. The first stage consisted of a 'pusher' sled, that housed 36 super Zuni rockets. The pusher sled was stopped by means of a water brake located 70 m from the ignition point. The second acceleration stage was provided by five Nike rockets which were attached directly to the F-4.

The target consisted of a block of reinforced concrete 7 m square and 3.66 m thick mounted atop an air-bearing platform with a combined weight of 469 tonnes (almost 25 times the weight of the F-4) (Figure 4). The target sat on top of a concrete slab that was cast immediately in front of a back-up structure. In order to calculate the impact force as a function of time, the magnitude of the friction between the target and the supporting concrete slab must be known. Because it is difficult to accurately estimate the friction between two rough, sliding surfaces, the friction between the two surfaces was reduced to an insignificant amount by a unique application of air bearings, which effectively supported the target on a thin layer of air. Ten air bearings were installed in "pockets" in the lower surface of the air-bearing platform. After inflating the air bearings, a force of only 816 Kg (less than 0.2% of the weight of the target) was required to initiate movement of the target. To ensure that the target (concrete block and the air-bearing platform) would move as a unit, a concrete lip was cast around the edges.

The details of the impact sequence (e.g. impact velocity, the process of deformation, and the possible detachment of the engines) were recorded with 16 high-speed framing cameras with frame rates varying from 500 to 2000

frames/second. The aircraft and the test panel were marked to aid in the reduction of the films. The high-speed photography was also used for an overall documentary of the test.

4 TEST RESULTS

4.1 Impact Velocity

A break-rod system on the track and an image-motion camera were used to measure the velocity of the aircraft just before impact. The break-rod system was installed near the end of the track. These break-rods were broken by the front shoe of the carriage structure as it passed by providing a unique signal on the recording device. In addition, the image of the aircraft was recorded on the film of the image-motion camera as a function of time as the aircraft passed by the field of view of the camera.

The data from these systems indicated on impact velocity of 215 m/s $\pm$ 1%.

4.2 Physical Damage to Aircraft and Target

The aircraft impacted the target at a perfectly normal orientation and was crushed from the front of the aircraft as shown in Figure 5. At impact a short portion of each wing tip and tail was sheared off. The remainder of the aircraft, from the nose to the tail, and the engines were completely destroyed during impact; pieces were found over a large area concentrated behind and to both sides of the target. The damage to the engines was very similar to that observed in the engine impact tests [6]. The dispersion of the water that simulated the fuel was relatively small.

Damage to the target was relatively minor indicating that the major portion of the impact energy went into movement of the target and not in producing structural damage (Figure 6). The face of the target was scarred where the aircraft fuselage hit, but only superficial damage was inflicted over this region. The penetration depth caused by the engines, which appear as the 'eyes' of the aircraft in the figure, was 60 mm at a maximum, and that caused by the fuselage was a maximum of 20 mm. The load damage caused by the fuselage is insignificant when compared with the damage due to the engines. Most of the damage was done by the carriage structure and the Nike rocket cases. The concrete spalled off the front face of the target from the level of the rocket case mounts and the carriage structure to within 150 mm of the bottom of the vertical panel. The target was displaced 1.83 m against the back-up structure and rebounded. Note that this impact did not occur until after all the data of interest had been obtained.

4.3 Target Response

Four displacement and velocity gages and five accelerometers were used at the rear face of the target to measure the motion of the target after impact (Figure 4). The displacement and velocity sensors were installed with 508 mm of travel. The accelerometers were installed at the same four positions; an additional accelerometer was located at the centroid of the target.

Some typical acceleration, velocity, and displacement measurements are shown in Figures 7-9. Also shown are the results of integration of the measured accelerations and velocities, which are in excellent agreement with the measured velocities and displacements, respectively (Figures 8, 9). The major acceleration began about 20 msec after impact and ended about 60 msec after impact. The velocity also began to increase rapidly after 20 msec, indicating that the major force was applied at about that time. The average velocity was nearly constant after 65 msec. This indicates that the impact force was

essentially zero after this time and the target continued to move in free motion until it impacted the back-up structure.

4.4 Onboard Sensor Response

Ten accelerometers were placed along the top of the fuselage of the aircraft (Figure 1) to acquire the decelerations as functions of time during the impact sequence. One accelerometer was also attached to the aft flange of each engine. A telemetry package that was mounted in the tail section of the aircraft was used to transmit the readings. Figure 10 shows the readings from station J10 on the fuselage and Figure 11 from station J13 on the left engine. Time integration of these decelerations provided the reduction in velocity versus time from initial impact until the sensors were destroyed. Red vertical stripes were painted on the fuselage at the same axial locations as the accelerometers. The differential crushing of the fuselage could then be examined from both the accelerometer measurements and the high-speed photography data.

Two methods were used to monitor the possible detachment of the engines before their impact. For the first method, the lower rear portion of the engine covers were removed. The exposed parts of the engines and the area of the fuselage just above the exposed portion of each engine were painted red with black vertical stripes. Close-up photographic coverage of this region of the aircraft during impact indicated no relative motion of either engine with respect to the fuselage. A total of four breakwire systems, which were installed between the engines and the fuselage, were housed to detect engine detachment. One set of breakwires was fastened to the outboard side of the rear end of each engine and one to the inboard side. Each set of breakwires were wired in a parallel circuit such that a break in a particular wire changed the circuit voltage by a given magnitude. The recorded failure times indicated that the engines did not move forward with respect to the fuselage prior to impact of the engines; however, at impact they were detached.

5 SUMMARY

This paper describes the impact test of a complete F-4 Phantom against a massive, rigid block of concrete which 'floated' on a set of air bearings. Extensive diagnostics were used to record the deceleration of the aircraft and the movement of the target. Discussion of the method used to calculate the impact force is given in a companion paper [5].

6 ACKNOWLEDGMENTS

The work was funded by Muto Institute of Structural Mechanics, Inc. and performed at Sandia National Laboratories, which is operated for the U.S. Department of Energy under Contract DE-AC04-76DP00789. At Sandia the effort by many individuals is gratefully acknowledged.

REFERENCES

1. Zorn, N. F., Riera, J. D., and Schüller, G. I., "On the Definition of the Excitation Due to Engine Impact," Proc. RILEM CEB IABSE IASS-Interass. Symposium, Concrete Structures under Impact and Impulsive Loading, Berlin, June 2-4, 1982, BAM (Bundesanstalt für Materialprüfung) May 1982, pp. 29-36.

2. Zorn, N. F., Schüller, G. I., and Riera, J. D., "A Probabilistic Approach for Evaluation of Load Time History of an Aircraft Impact," Proc. Int. Conf. Structural Mechanics in Reactor Technology, Paris, August 1981, pp. 1-7.

3. Riera, J. D., Zorn, N. F., and Schüeller, G. I., "An Approach to Evaluate the Design Load Time History for Normal Engine Impact Taking into Account the Crash-Velocity Distribution," Nuclear Engineering and Design, Vol. 71, 1982, pp. 311-316.

4. Riera, J. D., and Zorn, N. F., "Risk Due to Accidental Aircraft Crash Against Nuclear Power Plants: On the Definition of the Excitation Due to Engine Impact," Caderno Tecnico, CT28/81, 1981, Universidade Federal do Rio Grande do Sul, Porto Alegre, Brasil.

5. Muto, K., et al., "Full-Scale Aircraft Impact Test for Evaluation of Impact Forces, Part II, Analysis of Results," Proc. 10th SMiRT Conference.

6. Muto, K., et al., "Experimental Studies on Local Damage of Reinforced Concrete Structures by Deformable Missiles, Part 3: Full-Scale Tests," Proc. 10th SMiRT Conference.

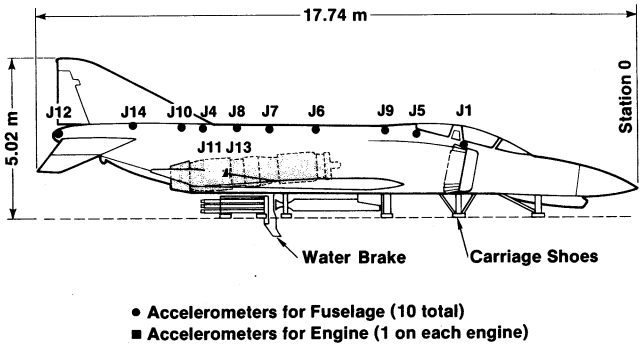

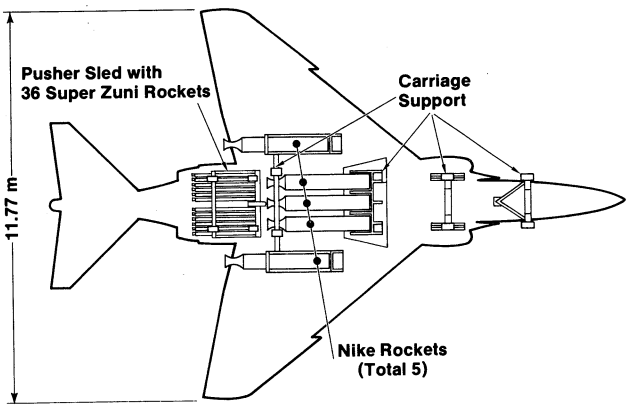

Fig. 1 F-4 Phantom Test Configuration

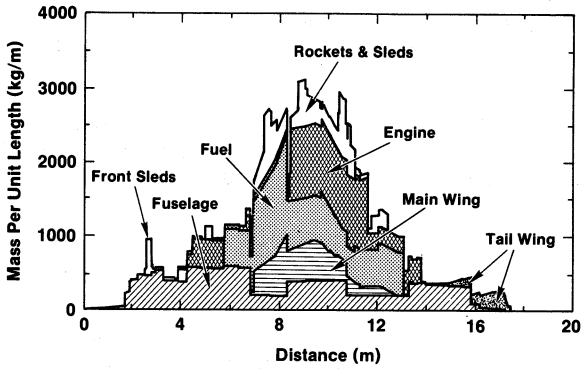

Fig. 2 Mass Distribution of F-4D for Impact Test

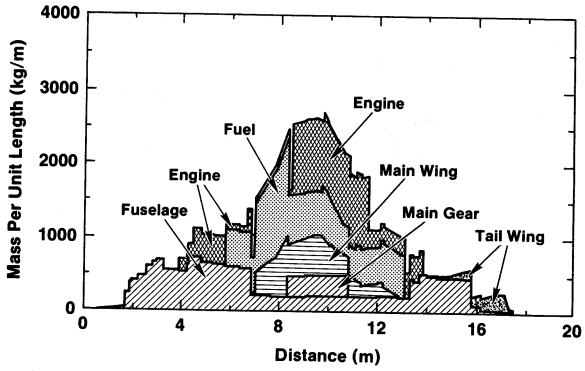

Fig. 3 Mass Distribution of an Original F-4D

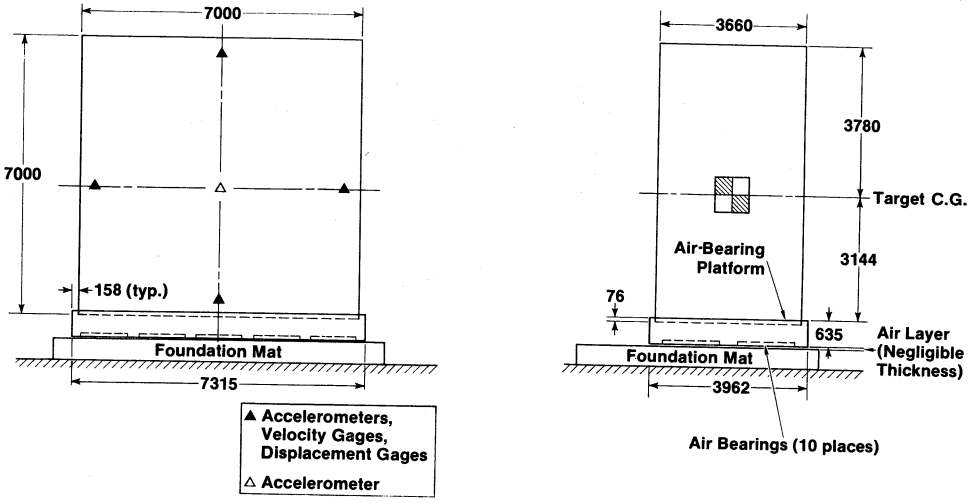

Fig. 4 Target

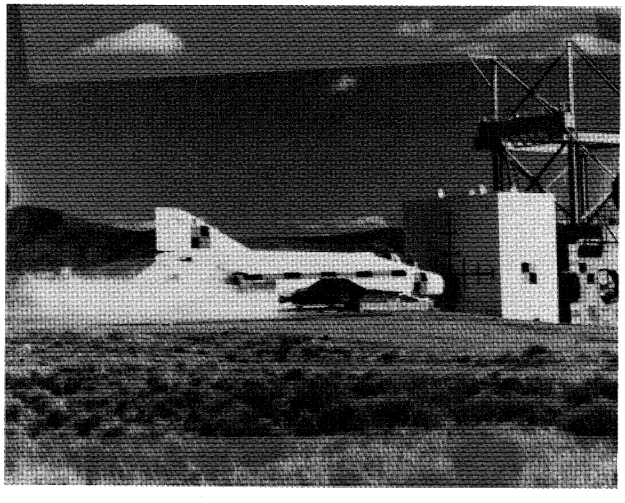

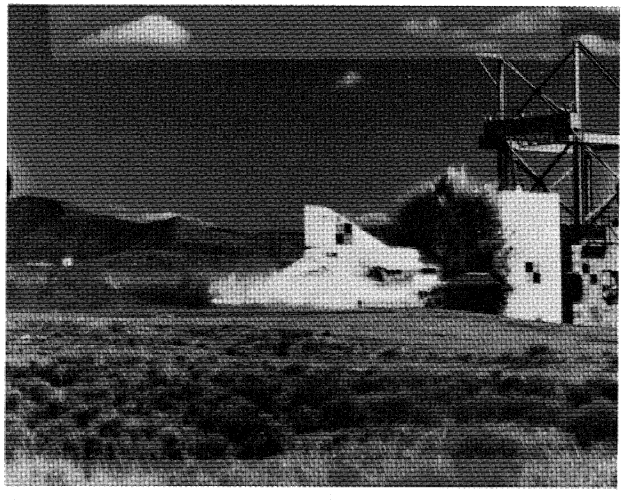

Fig. 5 Views of the Aircraft during Impact

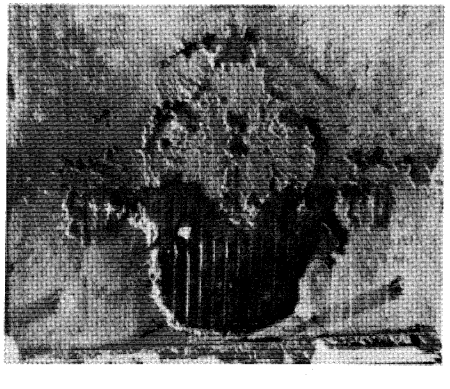

Fig. 6 Target Damage

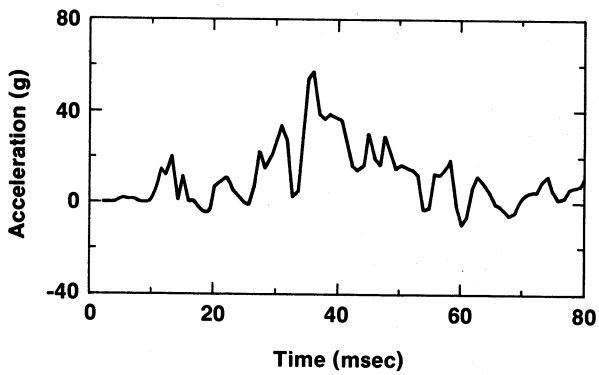

Fig. 7
Average of the Five Target
Acceleration Measurements

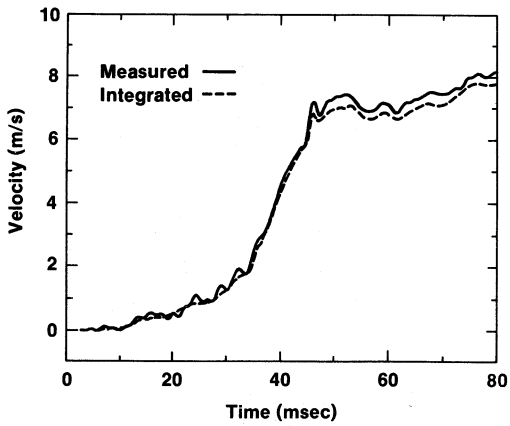

Fig. 8
Measured Velocity and Time Integrated
Acceleration at West Side of Target

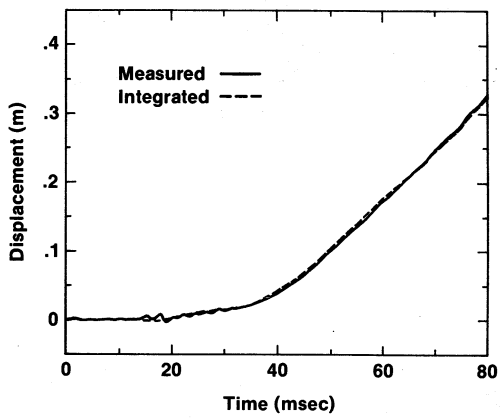

Fig. 9
Measured Displacement and Time Integrated Velocity at West Side of Target

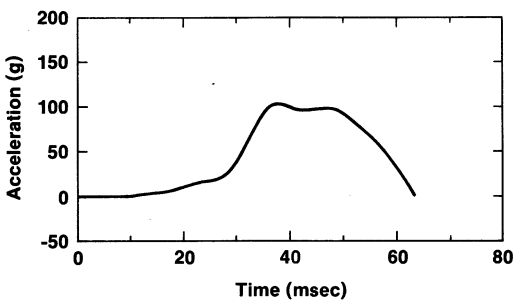

Fig. 10
Measured Acceleration at
Station J-10 on the Fuselage

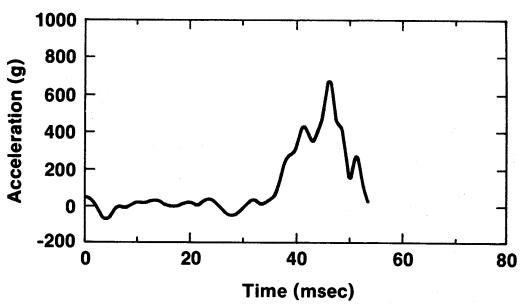

Fig. 11
Measured Acceleration at
Station J-13 on the Left Engine